Journal of Chemical Technology and Metallurgy, 59, 6, 2024, 1431-1436

FUNCTIONAL OPTICAL MATERIALS BASED ON AEROGELS

Dimitar Shandurkov, Nina Danchova, Stoyan Gutzov

Sofia University St. Kliment Ohridski
Faculty of Chemistry and Pharmacy
Department of Physical Chemistry
Sofia 1164, Bulgaria
E-mail: sgutzov@chem.uni-sofia.bg

Received 01 November 2023
Accepted 09 August 2024
DOI: 10.59957/jctm.v59.i6.2024.19

ABSTRACT

Sol-chemistry is an efficient physico-chemical method for the preparation of porous glassy or nanocrystalline materials with tailored electrical, thermal or optical properties. This paper focuses on the dependence preparation–structure-properties of hydrophobic silica aerogel granules, powders and composites with a potential application as optical materials. Using the technique of subcritical preparation of silica aerogel powders, multicolour emitting composites containing $Eu(phen)_2(NO_3)_3$ or $Tb(phen)_2(NO_3)_3$ nanocrystals are obtained and characterized with luminescence spectroscopy, quantum yield determination and texture measurements. A dependence of the luminescence quantum yield on the degree of hydrophobicity α of the silica aerogel powders is described.

Keywords: sol-gel, aerogel, europium, terbium, luminescence, hydrophobicity.

INTRODUCTION

Aerogels are highly porous materials that contain 95 % air in their structure with a wide popularity in recent decades. Their valuable properties, based on their unique structure such as low density, thermal insulation properties, transparency, make them attractive in many research areas [1]. Aerogels are included in part of NASA's projects for the development of materials applicable in space, in aircraft, insulation equipment, astronaut suits, blankets, etc. [2].

Along with their advantages and valuable properties, aerogels possess some disadvantages. Silica aerogel materials are brittle and do not have good plastic properties. This is the reason for the search for new modified aerogel materials that combine the advantages of the aerogel matrix and properties of the new component embedded in their structure, for example reinforced silica aerogels with a polymer component incorporated in the matrix [3].

Another new research direction of hybrid composites-based aerogels is the incorporation of optical active components into aerogel granules and powders. In this way, aerogel composite materials, which combine the properties both aerogel matrix and the embedded complex, are developed. Except a combination of the properties of both components (activator and sol-gel matrix), new properties resulting on the interaction between the individual components are expected [4]. In this way, attractive optical materials are prepared where the activator in the form of hybrid molecules or nanocrystals is immobilized in the pore system of the aerogels.

The sol-gel method is an attractive way used to prepare aerogels with tunable physical properties. There are several ways to prepare bulky aerogels, granules or powders: supercritical drying, subcritical drying, freeze drying or even 3D printing [5]. The subcritical drying method, allows the preparation of large amounts of hydrophobic silica aerogel granules and powders under

ambient pressure and room temperature [2]. This method consists of two additional step, applied to the wet silica gels, solvent exchange and subsequent hydrophobization which lead to widely used granules with controlled pore diameter, sizes and degree of hydrophobicity [6].

The aim of the present work is to summarize the optical properties of functional optical aerogel materials based on silica aerogel matrices, doped with $[Eu(phen)_2](NO_3)_3$ and $[Tb(phen)_2](NO_3)_3$ nanocrystals and to describe the texture properties of such composites.

EXPERIMENTAL

For the preparation of the aerogel composites an improved two-step colloidal route, based on the synthesis of silica aerogel powders, starting from tetraethylorthosilicate (TEOS) and their later functionalization, was used. During the preparation, after a room temperature solvent exchange with absolute ethanol, the wet silica gels were functionalized with trimethyl chlorosilane (TMCS) to achieve powders with a different degree of hydrophobicity.

In the first step a composite SiO_2:$Ln(NO_3)_3$ was formed (Ln = Eu or Tb), which is later functionalized with a 1,10 - phenanthroline (phen) solution in ethanol. In this way, the poor solubility of the Ln-phen complexes in ethanol was utilized and nanocrystallites are formed in situ in the pores of the gel and micrometer scaled powders with a different degree of hydrophobicity α were obtained [7, 8]. The degree of hydrophobicity α is defined as the molar ratio between TMCS and TEOS ($\alpha = n_{TMCS} / n_{TEOS}$). [6]. All the samples were dried in a vacuum oven NÜVE with a volume of 15,000 cm^3 at room temperature and constant pressure of about 100 mbar. The amount of the Ln activators in all samples was $n_{Ln} / n_{Si} = 0.0035$.

The luminescence and excitation spectra of the red or green emitting samples were recorded on a fluorimeter PE FL 8500, equipped with an integrating sphere (N4201017) for absolute quantum yield (QY) measurements. All samples were placed in a 1 cm quartz cell for the QY measurements. The absolute QY was achieved using the calculation method of Suzuki et al. with an error of about 5 % [9]. Emission and excitation spectra were recorded on the same fluorimeter using a variable angle solid sample holder. The spectra were measured under the same spectroscopic conditions / angle, slits and excitation power/.

The texture characteristics of the aerogel powders were determined by low-temperature (77.4 K) nitrogen adsorption-desorption isotherms in a Quantachrome Instruments NOVA 1200e (USA) instrument. The following parameters were calculated from the isotherms: the specific surface areas (S_{BET}) were determined based on the BET equation, the total pore volumes (V_t) and associated average pore diameters (D_{av}) were estimated at a relative pressure close to 1. All samples were outgassed and dried from leftover solvents for 16 h in vacuum at 150°C before the measurements.

RESULTS AND DISCUSSION

Preparation - properties relationships of the hybrid composites

The aim of the physico-chemical preparation strategy in this contribution is the incorporation of optically active nanocrystals, $[Ln(phen)_2](NO_3)_3$, into the amorphous silica aerogel matrix. The luminescence of such composites is based on the luminescent properties of the lanthanide (Ln) ions, terbium (III) and europium (III), with their typical sharp, weak f-f emission lines in the visible and IR spectral region at UV excitation. The availability of 15 - 20 nm $[Ln(phen)_2](NO_3)_3$ nanocrystals in the amorphous silica composites is detected with powder X-Ray diffraction [10].

The quantum yield of the Ln(III) emission is increased by an energy transfer in hybrid molecules, realized by the well-known Förster energy transfer mechanism, its efficiency strongly depending on the physical nature of the ligands (energy of the singlet and triplet state), also on the ligand to Ln ion distance and the spectral overlap. The UV - energy is absorbed by an organic molecule, for example 1,10 - phenathroline, β-diketonates, acetic acid, acethylacetone, aromatic molecules and other compounds and transferred to the Ln - activator ion [11].

Excitation and emission spectra

The excitation spectra of the aerogel composites (Fig. 1 and Fig. 2) confirm that a strong, effective energy transfer takes place at UV excitation. There are three main excitation channels, one at about 260 nm, together with two strong excitation pathways at about 310 nm and 355 nm, coming from Forster Resonant Energy Transfer

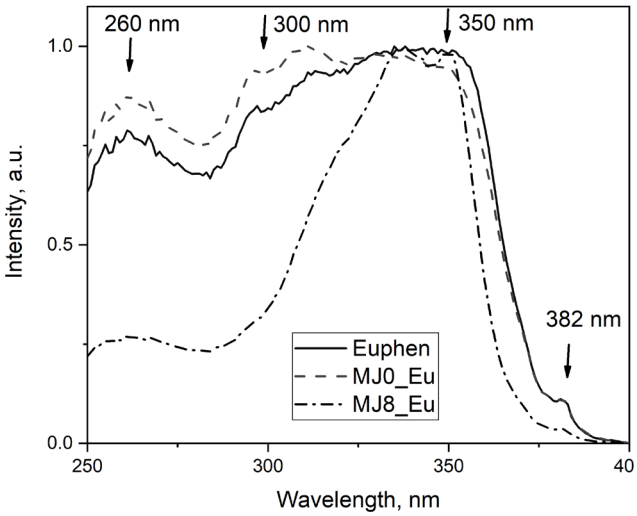

Fig 1. Excitation spectra (at 615 nm emission) of aerogel composites, prepared from aerogel powders with a different degree of hydrophobicity, α. The spectra are compared to that of the pure solid complex $[Eu(phen)_2](NO_3)_3$, euphen. The excitation channels are visible.

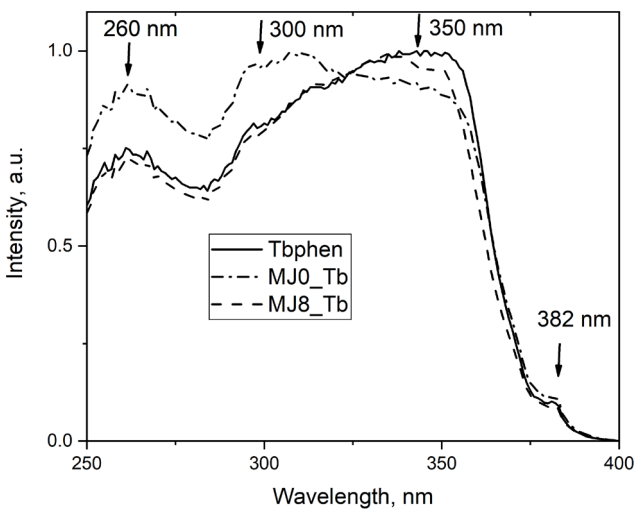

Fig. 2. Excitation spectra (at 542 nm emission) of aerogel composites, prepared from aerogel powders with a different degree of hydrophobicity, α. The spectra are compared to that of the pure solid complex $[Tb(phen)_2](NO_3)_3$, tbphen. The excitation channels are visible.

($S_0 \rightarrow S_1 \rightarrow T_1 \rightarrow {}^5D_J$) in the 1,10 - phenathroline molecule [12]. Here, ${}^5D_J$, denotes the excited energy level of the Ln ions. The direct excitation of the f-ions takes places with a low intensity at about 380 nm.

In the case of Eu(III) the relative intensities of the excitation peaks are similar for composites with α = 0 and the pure solid complex, while the spectrum of powders with α = 1.407 has a very weak excitation peak at 260 nm. The observation is close to that of dense, hydrophilic sol-gel silica composites, containing $[Eu(phen)_2](NO_3)_3$ with $n_{Eu} / n_{Si} = 0.05$ [10, 13]. The excitation spectrum of the pure, solid complex $Tb(phen)_2(NO_3)_3$, however, is close to that of composites with α = 1.407, while composites with α = 0 display a stronger band at 260 nm.

The excitation spectra in Fig. 1. and Fig. 2. prove a complicated excitation channel structure of the $[Ln(phen)_2](NO_3)_3$ nanocrystals, embedded in the pores of the aerogel granulates. The observation is in contradiction with simplified theoretical expectations, where only two excitation channels of Tb and Eu 1,10-phehnathroline complexes in hydrophobic or hydrophilic silica, at 245 nm and 355 nm are presented [14].

As is pointed out, the excitation spectra in this contribution suggest a complicated energy transfer scheme, probably including a charge transfer transition (CTT) at 260 nm. From a general chemical point of view, a ligand to metal CTT from the 1,10 - phenanthroline molecule to the Ln(III) ion is less probable. Metal – to ligand charge transfer transitions involving the 1,10 - phenanthroline molecule and cuprum ions, however, are well known and even used in optical technologies [15 - 17]. The oxidation state of europium and terbium in this contribution does not favor a metal to ligand CTT.

Another explanation for the different relative intensity of the 260 nm band here could be a charge transfer transition, $O^{2-} \rightarrow Ln^{3+}$, including the oxygen ions of the silica pore walls of the matrix or from the NO_3 groups coordinated around the lanthanide ion. Such an assumption needs a chemical interaction between the activator nanocrystals and the silica matrix at a nanoscale and needs additional spectroscopic and diffraction investigations. More about the thermodynamics of the silica phases are summarized in [18]. The occurrence of the $O^{2-} \rightarrow Ln^{3+}$ in rare earth ion containing inorganic luminescent materials has been widely used in lighting technologies [12]. Not least, the silica sol-gel matrix contains a variety of electronic defects with a significant

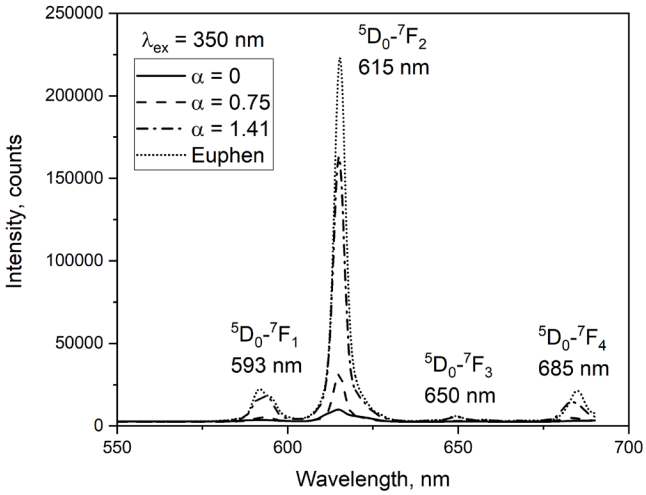

Fig.3. Luminescence spectra of red emitting composites, prepared from aerogel powders with a different degree of hydrophobicity α, compared to that of the pure solid complex $[Eu(phen)_2](NO_3)_3$, Euphen. The f-f electronic transitions of the Eu^{3+} are shown.

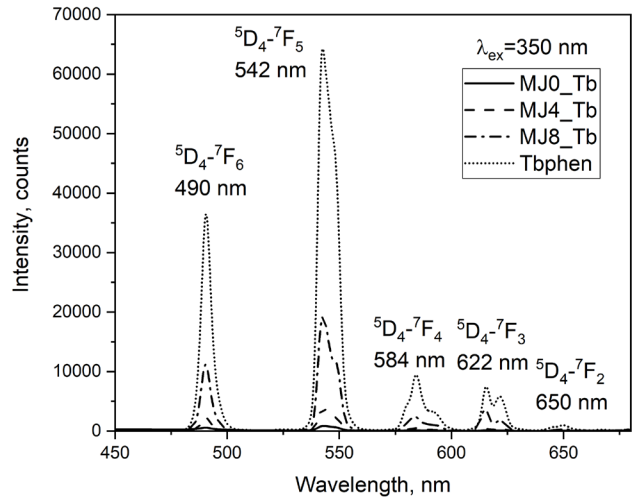

Fig. 4. Luminescence spectra of green emitting composites, prepared from aerogel powders with a different degree of hydrophobicity α, compared to that of the pure solid complex $[Tb(phen)_2](NO_3)_3$, Tbphen. The f-f electronic transitions of the Tb^{3+} ion is shown.

role in the relative UV excitation peaks intensity of dense SiO_2:Tb,Ce gels [19]. The excitation spectra (Fig. 1 and Fig. 2) show that the relative excitation peak intensities also depend on the degree of hydrophobicity α of the initial aerogel matrix and on the type of the activator ion.

The emission spectra of the composites investigated are presented on Fig. 3 and Fig. 4. They contain sharp lines, typical for the f-f transitions of the Eu(III) and Tb(III) ions. The site-symmetry of the lanthanide ions is low, C_{2V} or lower, according to the spectra - structure correlation of the europium ion in different crystalline environment and crystallographic data of the pure, solid $[Ln(phen)_2](NO_3)_3$ complexes [12, 20]. It is visible, that at the same excitation wavelength the composites response with a green or red emission, depending on the f-f doping agent. In other words, the way for "smart" sensors based on $[Ln(phen)_2](NO_3)_3$ nanocomposites or with photoluminescence at 350 nm excitation is still open.

Fig. 4. presents the luminescence spectra of aerogel like silica powders, doped with $[Tb(phen)_2](NO_3)_3$ nanocrystals. As is the case of the red emitting composites, the luminescence intensity depends on the degree of hydrophobicity of the initial aerogel powder. The peak maxima in Fig. 3. and Fig. 4. corresponds very well to the f-f electronic transitions of the Eu^{3+} and Tb^{3+} ions [12].

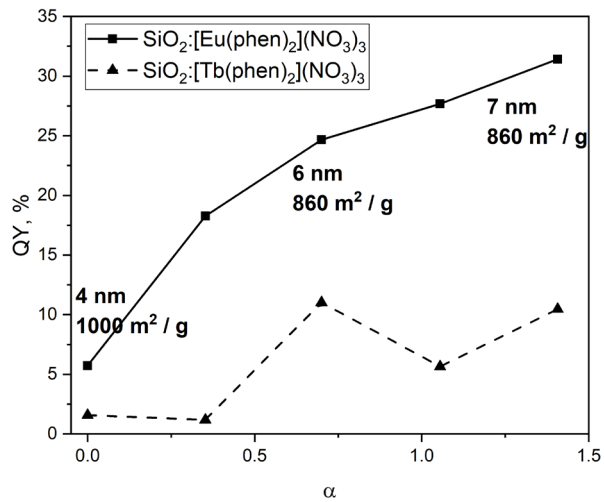

Fig. 5. Quantum yield of the red and green emission of aerogel composites, depending on the degree of hydrophobicity α of the initial aerogel powders. The texture properties of the initial aerogel powders D_{AV} [nm] and S_{BET} [m^2 g^{-1}] are shown. The n_{Ln} / n_{Si} of all samples is 0.0035.

Quantum yield and texture properties of the initial aerogel powders and doped composites.

The quantum yield (QY) vs. α dependence is visualized in Fig. 5. The values of the QY are taken from [10]. Here, texture data of the initial aerogel matrix added also are shown. At high degrees of hydrophobicity of the initial aerogel powders the

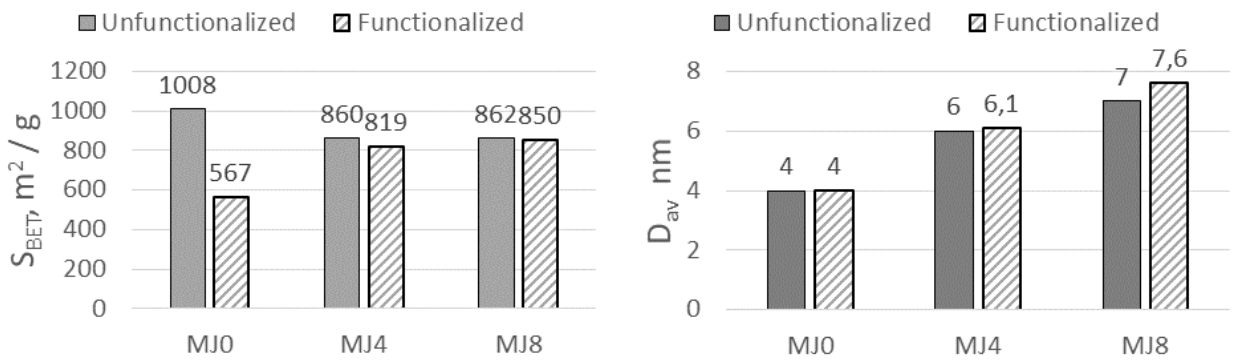

Fig. 6. Texture properties of functionalized with $Eu(phen)_2(NO_3)_3$ nanocrystals and unfunctionalized aerogel powders with a different degree of hydrophobicity, α. Notations: MJ0 – α = 0; MJ4 – α = 0.7; MJ8 – α = 1.4; S_{BET} - specific surface areas, Dav - average pore diameters.

quantum yield is close to that of the pure solid complexes. Samples with α = 0 emit very weak with a low quantum yield.

Beside the f-f luminescence of the Eu and Tb ions, a weak blue emission with a maximum at 420 nm and a quantum yield lower than 1 % is detected in composites, produced from aerogels with a low degree of hydrophobicity, α < 0.4. This emission is connected with the occurrence of nanocrystals of 1,10 - phenanthroline in the nanopores of the silica matrix. The quantum yield of the blue emission is no presented in Fig. 5. The crystal structure of the monoclinic $[Ln(phen)_2](NO_3)_3$ is also given [21 - 23].

Fig. 5. proves, that the most important factor for the increasing quantum yield of the red and green emission of the silica aerogel composites is the degree of hydrophobicity of the initial aerogel powder, while the texture properties of all samples are similar. A probable explanation of this observation is that the hydrophobization with TMCS removes the OH groups from the silica surface of the aerogel powders. Hydroxyl groups are an inhibitor of the luminescence intensity of f-ions because of the increase of nonradiative electronic transitions [12]. In the case of powders with a very high specific surface, as is the case of aerogel powders, the amount of surface OH groups is high and their action becomes dominating.

The texture properties of the doped aerogel samples are summarized in Fig. 6. Here, the nitrogen adsorption-desorption analysis results for the specific surface area S_{BET} and the average pore sizes D_{AV} of initial and functionalized with $[Eu(phen)_2](NO_3)_3$ aerogel powders are presented.

It is visible, that the functionalization with $[Eu(phen)_2](NO_3)_3$ nanocrystals does not change significantly the texture properties of hydrophobic aerogel powders. In the case of hydrophilic powders, however, the decrease of the specific surface area S_{BET} is significant. A possible explanation of the observation is that the bottle-like pores of the hydrophilic composites are obstructed at the entrance by the formed luminescent nanocrystals. A detailed analysis of the pore structure and morphology of hydrophilic and hydrophobic silica aerogels, on the basis of the BET equation, is performed by Shandurkov et al. [6].

CONCLUSIONS

Aerogel granules or nano powders with promising physical properties are prepared by a laboratory subcritical approach at room temperature and p = 0.1 atm. A new laboratory method for functionalization of silica aerogel granules with organic ligands is demonstrated. The quantum yield of the optical composites strongly depends on the degree of hydrophobicity of the initial aerogel powders. The relative excitation peak intensities of the aerogel composites depend on the degree of hydrophobicity α of the initial aerogel matrix and on the type of the activator ion. Functionalization with $[Ln(phen)_2](NO_3)_3$ nanocrystals does not change significantly the texture properties of the hydrophobic aerogel granules.

Acknowledgements

The authors thank the Project CoE "National center of mechatronics and clean technologies" BG05M2OP001-1.001-0008-C01 for the financial support. The paper is a tribute to Professor Ivan S. Gutzow (1933 - 2020), Full Member of BAS.

REFERENCES

1. C. Brinker, G. Scherer, Sol-gel science, Academic press, 1990.
2. M.A. Aegerter, N. Leventis, M.M. Koebel, Aerogels Handbook, Springer, New York, 2011. https://doi.org/https://doi.org/10.1007/978-1-4419-7589-8.
3. P. Gomez-Romero, C. Sanchez, Functional Hybrid Materials, Wiley-VCH, 2003. https://doi.org/10.1002/3527602372.
4. Sol-Gel Process, (n.d.). http://www.chemat.com/chemattechnology/SolGel.aspx.
5. I. Binyamin, E. Grossman, M. Gorodnitsky, D. Kam, S. Magdassi, 3D Printing Thermally Stable High-Performance Polymers Based on a Dual Curing Mechanism, Adv. Funct. Mater., 33, 2023, 2214368.
6. D. Shandurkov, P. Ignatov, I. Spassova, S. Gutzov, Spectral and Texture Properties of Hydrophobic Aerogel Powders Obtained from Room Temperature Drying, Molecules, 26, 2021, 1796. https://doi.org/10.3390/molecules26061796.
7. S.S. Kistler, Coherent Expanded-Aerogels, J. Phys. Chem., 36, 1932, 52-64. https://doi.org/DOI: 10.1021/j150331a003.
8. S.S. Kistler, Coherent Expanded Aerogels and Jellies, Nature., 127, 1931, 741. https://doi.org/doi:10.1038/127741a0.
9. K. Suzuki, A. Kobayashi, S. Kaneko, K. Takehira, T. Yoshihara, H. Ishida, Y. Shiina, S. Oishi, S. Tobita, Reevaluation of absolute luminescence quantum yields of standard solutions using a spectrometer with an integrating sphere and a back-thinned CCD detector, Phys. Chem. Chem. Phys., 11, 2009, 9850-9860. https://doi.org/10.1039/b912178a
10. S. Gutzov, D. Shandurkov, N. Danchova, V. Petrov, T. Spassov, Hybrid composites based on aerogels: preparation, structure and tunable luminescence, J. Lumin., 251, 2022, 119171.
11. R. Hull, J.R.M. Osgood, J. Paris, H. Warlimont, Spectroscopic properties of Rare Earths in Optical Materials, Springer, 2014.
12. G. Blasse, B.C. Grabmaier, Luminescent Materials, Springer-Verlag, Telos, 1994.
13. S. Gutzov, D. Shandurkov, N. Danchova, D. Enseling, T. Jüstel, Preparation and optical properties of functionalized hydrophobic aerogel granules, SPIE Proc., 11332, 2019. https://doi.org/10.1117/12.2552727.
14. T. Zahariev, N. Trendafilova, I. Georgieva, Spectroscopic and photophysical properties of [Eu(Phen)2]X3 (X ≡ Cl–, NO_3–) complexes, incorporated into SiO_2-based Matrices: Theoretical study, Mater. Today Proc., 61, 2022, 1292-1299.
15. V. Scaltrito, D.W. Thompson, J.A. O'Callaghan, G.J. Meyer, MLCT excited states of cuprous bis-phenanthroline coordination compounds, Coord. Chem. Rev., 208, 2000, 243-266.
16. J.L. Barilone, J. Tůma, S. Brochard, K. Babková, M. Krupička, Design of Bis(1,10-phenanthroline) Copper(I)-Based Mechanochromic Indicators, ACS Omega, 7, 2022, 6510-6517.
17. J. Wu, M. Alías, C. de Graaf, Controlling the Lifetime of the Triplet MLCT State in Fe(II) Polypyridyl Complexes through Ligand Modification, 8, 2020.
18. I.S. Gutzow, J.W.P. Schmelzer, The vitreous State, Springer Verlag, 1994.
19. S. Gutzov, M. Bredol, Optical properties of cerium and terbium doped silica xerogels, J. Mat. Sci., 46, 2006, 1835-1837.
20. J.G. Bünzli, The europium(III) ion as spectroscopic probe in bioinorganic chemistry, Inorganica Chim. Acta, 139, 1987, 219-222.
21. A.G. Mirochnik, B. V. Bukvetskii, P.A. Zhikhareva, V.E. Karasev, Crystal Structure and Luminescence of the [Eu(Phen)2(NO3)3] Complex. The Role of the Ion-Coactivator, Russ. J. Coord. Chem., 27, 2001, 443-448.
22. I.V. Taidakov, B.E. Zaitsev, A.N. Lobanov, A.G. Vitukhnovskii, Z.A. Starikova, Synthesis and crystal structure of the Tb(III) complex with 1,3-bis(1,3-dimethyl-1H-pyrazol-4-yl)-1,3-propanedione and 1,10-phenanthroline, Russ. J. Coord. Chem., 38, 2012, 300-304.
23. T. Zahariev, D. Shandurkov, S. Gutzov, N. Trendafilova, D. Enseling, T. Jüstel, I. Georgieva, Phenanthroline chromophore as efficient antenna for Tb^{3+} green luminescence: A theoretical study, Dye. Pigment., 185, 2020, 108890.